Layer undulations in a smectic C liquid crystal with weak anchoring

2007 J. Phys. A: Math. Theor. 40 11849

(http://iopscience.iop.org/1751-8121/40/39/010)

IOP PUBLISHING JOURNAL OF PHYSICS A: MATHEMATICAL AND THEORETICAL

J. Phys. A: Math. Theor. **40** (2007) 11849–11861 doi:10.1088/1751-8113/40/39/010

Layer undulations in a smectic C liquid crystal with weak anchoring

A J Walker and I W Stewart

Department of Mathematics, University of Strathclyde, Livingstone Tower, 26 Richmond Street, Glasgow, G1 1XH, UK

E-mail: ta.awal@maths.strath.ac.uk and i.w.stewart@strath.ac.uk

Received 21 May 2007, in final form 16 August 2007
Published 11 September 2007
Online at stacks.iop.org/JPhysA/40/11849

Abstract

The free energy for a sample of smectic C liquid crystal bounded between two semi-infinite plates with weak surface anchoring on the boundaries is considered. A magnetic field is applied across the sample and the ensuing layer undulations are studied. The free energy is minimized to give relations involving the elastic energies, magnetic field strength and wave numbers which govern the layer undulations. Forms for the critical field strength and critical wave numbers are derived and compared to analogous results in a system with strong surface anchoring. An expression for the layer undulation amplitude is derived for weak anchoring which can be compared with the classical Helfrich–Hurault theory for strong anchoring and recent experimental results for cholesteric liquid crystals.

PACS numbers: 61.30.−v, 61.30.Dk

1. Introduction

This paper is concerned with field-induced layer undulations on smectic C (SmC) liquid crystals confined between two flat plates. Layer undulations (which are related to buckling) in liquid crystals occur since curvature deformations are capable of relaxing dilation or field-induced stress. The phenomena can be described as follows. The smectic liquid crystal is confined between two plates, which are parallel to the smectic layers and a magnetic field is applied across the sample, parallel to the smectic layers, causing the layers to reorient if the magnetic field is above some critical field strength H_c. Since the surface anchoring on the plates does not allow the layers to tilt freely, an undulation of the layers is observed.

We consider a model for the onset of layer undulations in SmC liquid crystals subject to an applied magnetic field with a weak-anchoring energy at the boundaries. There are well known theoretical results which determine a critical magnetic field magnitude H_c for the onset of layer undulations in infinite samples of smectic A (SmA) where the transition from uniformly aligned planar layers to undulated layers is known as the Helfrich–Hurault

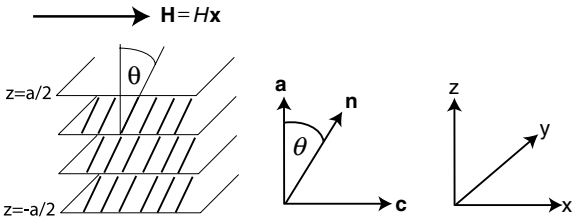

Figure 1. Schematic arrangement of a planar aligned sample of SmC liquid crystal described in Cartesian coordinates. The director **n** is tilted at an angle θ to the layer normal **a**; **c** is the unit orthogonal projection of **n** onto the smectic planes. A magnetic field **H** of magnitude H is applied in the x-direction. The director is subject to weak anchoring on the upper and lower boundary plates at $z = \pm a/2$.

transition [1, 2]. Extensions to this work for SmA have been made by, among others, Fukuda and Onuki [3], Singer [4] and Stewart [5]. The derivation of critical field magnitudes for infinite samples of SmA can be found in the books by Chandrasekhar [6] and de Gennes and Prost [7]. An extension of this work from SmA to SmC has been carried out by Stewart [8] where a free energy has been constructed in terms of the displacement of the layers, denoted by u. However, all of these modifications assume that the undulations of the layers vanish at the cell boundaries, i.e. the smectic layers are assumed fixed by infinitely strong surface anchoring at the boundaries.

Motivated by the experimental and theoretical results on cholesteric liquid crystals by Ishikawa and Lavrentovich [9] and Senyuk *et al* [10], we construct a model of a SmC liquid crystal cell, with weak anchoring at the cell boundaries and with an applied magnetic field across the sample in the direction parallel to the boundary plates and the smectic layers, given schematically by figure 1. In section 2, the free energy of such a system is constructed and then minimized using a Gâteaux variation to produce, when a suitable layer displacement ansatz is supposed, relations involving the elastic energies, magnetic field strength and wave numbers which govern the layer undulations. Forms for the critical field strength and critical wave numbers are then derived using the free energy and the aforementioned relations and are then compared to analogous results in a system with strong surface anchoring in figure 2. We derive a form for the layer displacement amplitude in section 3 by comparing the free energy at criticality with the post-transitional free energy. Comparisons with cholesteric experiments [9] and the classical SmA theory are made in figures 3 and 4, respectively. Appropriate distinctions between the cholesteric results in [9] and the SmC results presented here will be made. Comments on the influence of the weak-anchoring energy density used to describe the interactions at the cell boundaries will also be highlighted. A brief discussion, in section 4, mentions that the techniques used in section 2 may be applicable to other smectic and lamellar models.

Liquid crystals are anisotropic fluids made up of elongated molecules whose average molecular axes align along a common direction in space which is usually denoted by the unit vector **n**, called the director. It is known that SmC liquid crystals form locally equidistant parallel layers in which the director **n** generally makes a fixed constant angle θ (the smectic tilt angle) with respect to the layer normal. The SmA phase occurs when $\theta \equiv 0$. Following de Gennes and Prost [7], SmC can be described by introducing the unit layer normal **a** and a vector **c**, which is the unit orthogonal projection of **n** onto the smectic planes, as shown in figure 1. The director **n** is related to **a** and **c** via the relation

$$\mathbf{n} = \mathbf{a}\cos\theta + \mathbf{c}\sin\theta. \tag{1.1}$$

It is also mathematically convenient to introduce the unit vector **b** defined by

$$\mathbf{b} = \mathbf{a} \times \mathbf{c}. \tag{1.2}$$

The nine-term bulk elastic energy integrand w_b for a non-chiral SmC liquid crystal can be written in terms of the derivatives of **a** and **c** as [11]

$$\begin{aligned} w_b = {} & \tfrac{1}{2}A_{21}(\nabla \cdot \mathbf{a})^2 + \tfrac{1}{2}B_2(\nabla \cdot \mathbf{c})^2 + \tfrac{1}{2}B_1(\mathbf{a} \cdot \nabla \times \mathbf{c})^2 \\ & + \tfrac{1}{2}B_3(\mathbf{c} \cdot \nabla \times \mathbf{c})^2 + \tfrac{1}{2}(2A_{11} + A_{12} + A_{21} + B_3)(\mathbf{b} \cdot \nabla \times \mathbf{c})^2 \\ & - \tfrac{1}{2}(2A_{11} + 2A_{21} + B_3)(\nabla \cdot \mathbf{a})(\mathbf{b} \cdot \nabla \times \mathbf{c}) - C_2(\nabla \cdot \mathbf{a})(\nabla \cdot \mathbf{c}) \\ & - B_{13}(\mathbf{a} \cdot \nabla \times \mathbf{c})(\mathbf{c} \cdot \nabla \times \mathbf{c}) + (C_1 + C_2 - B_{13})(\nabla \cdot \mathbf{c})(\mathbf{b} \cdot \nabla \times \mathbf{c}), \end{aligned} \tag{1.3}$$

where the nine elastic constants A_i, B_i and C_i are related to those introduced by the Orsay group [12], with the minor modifications $A_{11} = \frac{1}{2}A_{11}^{\text{Orsay}}$ and $C_1 = -C_1^{\text{Orsay}}$.

The magnetic energy density, ignoring a contribution which is independent of the orientation of **n**, may be written as [7]

$$w_m = -\tfrac{1}{2}\mu_0 \Delta\chi (\mathbf{n} \cdot \mathbf{H})^2, \tag{1.4}$$

where **H** is the magnetic field, μ_0 is the permeability of free space and $\Delta\chi$ (in SI units) is the magnetic anisotropy of the liquid crystal. The director is attracted to be parallel to the applied field when $\Delta\chi > 0$.

2. Energy analysis, criticality and weak-anchoring effects

In section 2.1, we construct the relevant energy densities before investigating the first variation in section 2.2. The influence of anchoring strength upon critical wave numbers and field strengths will be presented. The strong-anchoring limit will be discussed in section 2.3.

2.1. Bulk and surface energies

We construct the relevant free energy for the system detailed in the introduction and figure 1, with particular reference to the smectic layer displacement function. Smectic layers are surfaces which can be represented by a layer function Φ of the form

$$\Phi(x, y, z) = \text{constant}, \tag{2.1}$$

so that the unit layer normal can be written as

$$\mathbf{a} = \frac{\nabla\Phi}{|\nabla\Phi|}. \tag{2.2}$$

We shall assume that, for small distortions, $\Phi = \Phi(x, z)$ so that there is no y-dependence in u, a simplification also made by de Gennes and Prost [7] and Stewart [8, 13]. Under these circumstances, we can introduce a displacement u of the layers so that $u \equiv 0$ would give, in the geometry of figure 1, $\Phi = z$ and $\mathbf{a} = (0, 0, 1)$. It can then be supposed that the layer function may be written as [8]

$$\Phi = z - u(x, z). \tag{2.3}$$

Following the methodology in [8], **a** and **c** can then be calculated as (working to second order in u and its first derivatives)

$$\mathbf{a} = \left(-u_{,x}(1 + u_{,z}), 0, 1 - \tfrac{1}{2}u_{,x}^2\right), \tag{2.4}$$

$$\mathbf{c} = \left(1 - \tfrac{1}{2}u_{,x}^2, 0, u_{,x}(1 + u_{,z})\right), \tag{2.5}$$

from which it follows that $\mathbf{b} = (0, 1, 0)$.

In the absence of dislocations, the smectic layer normal satisfies $\nabla \times \mathbf{a} = \mathbf{0}$, a requirement that was first identified by Oseen [14] for SmA liquid crystals and which is also valid for SmC liquid crystals. However, as the smectic layers distort this requirement cannot generally hold, even for small displacements, and we note that the expression for $\mathbf{a}$ in (2.4) only satisfies this requirement to first order in u and its derivatives. If Φ changes slightly at the onset of deformations and we assume a constant density then we expect a contribution to a layer compression energy, in the present geometry, of the form [15]

$$w_L = \tfrac{1}{2} B_0 \big(u_{,z} - \tfrac{1}{2} u_{,x}^2\big)^2, \tag{2.6}$$

where $B_0 > 0$ denotes the smectic layer compression constant, having dimensions of energy per unit volume. We note here that w_L does not obey the transformation $u \to -u$ symmetry requirement. However, from the cholesteric experimental work of Ishikawa and Lavrentovich [16], the contribution entering through the derivative $u_{,z}$ is considered to be weak and therefore (2.6) retains enough rotation invariance to correctly describe the layer energy at this level of approximation. Considering the layer displacement term as a function that is independent of y further allows us to consider a simplified quadratic-order version of the bulk elastic energy stated at equation (1.3), given by

$$w_b = \tfrac{1}{2} A_{12} u_{,xx}^2 + \tfrac{1}{2} B_2 u_{,xz}^2 + (B_{13} - C_1) u_{,xx} u_{,xz}. \tag{2.7}$$

In the geometry of figure 1, the magnetic field takes the form

$$\mathbf{H} = H(1, 0, 0), \qquad H = |\mathbf{H}|. \tag{2.8}$$

Employing the forms for $\mathbf{a}$ and $\mathbf{c}$ given by (2.4) and (2.5) allows us to expand the magnetic energy density (1.4) to quadratic order in u and its derivatives to find

$$w_m = -\tfrac{1}{2} \mu_0 \Delta\chi H^2 \big(u_{,x}^2 \cos 2\theta - u_{,x}(1 + u_{,z}) \sin 2\theta + \sin^2\theta\big). \tag{2.9}$$

As a magnetic field is applied across the sample, it is anticipated that the angle between the normal to the boundaries and the director will change at the boundary due to the supposed weak-anchoring conditions. Such anticipated boundary behaviour must lead to the introduction of an additional surface energy corresponding to what is commonly called a weak-anchoring energy. The simplest such surface energy density is of a form first proposed by Rapini and Papoular [17] and can be written as [13]

$$w_s = \tfrac{1}{2} \tau_0 (1 + \omega(\mathbf{n} \cdot \boldsymbol{\nu})^2), \tag{2.10}$$

with $\tau_0 > 0$, $\omega > -1$ and $\boldsymbol{\nu}$ is the unit outward normal to the boundary surfaces. The constant ω is a dimensionless measure of the anchoring strength while τ_0 has the dimensions of energy per unit area. Using the definition of the director and the forms of the layer normal and the orthogonal projection of the director given in equations (1.1), (2.4) and (2.5), respectively, we may compute the surface energy density at each boundary (where $\boldsymbol{\nu}_\pm = (0, 0, \pm 1)$) so that it is given by

$$w_s = \tfrac{1}{2} \tau_0 + \tfrac{1}{2} \tau_0 \omega \big(\cos^2\theta - u_{,x}^2 \cos(2\theta) + u_{,x}(1 + u_{,z}) \sin(2\theta)\big), \tag{2.11}$$

where we have neglected powers of u and its derivatives of orders three and above.

The free energy integral can now be written in the form

$$F = \int_\Omega (w_L + w_b + w_m)\, \mathrm{d}\Omega + \int_S w_s\, \mathrm{d}S, \tag{2.12}$$

where Ω is the region in which the magnetic field is applied, S is the surface region in which the surface energy acts and the integrands w_L, w_b, w_m and w_s are the layer compression energy, the bulk elastic energy, the magnetic energy and the weak-anchoring surface energy given by

equations (2.6), (2.7), (2.9) and (2.11), respectively. We assume periodicity along the x-axis with period $2\pi/q_x$ and suppose that the liquid crystal is confined in the geometry of figure 1 so that the centre of the sample is at $z = 0$ and the cell has depth a. Hence the free energy per unit length in y and over one period in x is

$$F = \int_0^{\frac{2\pi}{q_x}} \int_{-\frac{a}{2}}^{\frac{a}{2}} (w_L + w_b + w_m)\,\mathrm{d}z\,\mathrm{d}x + \int_0^{\frac{2\pi}{q_x}} \left([w_s]_{z=-\frac{a}{2}} + [w_s]_{z=\frac{a}{2}}\right)\mathrm{d}x. \tag{2.13}$$

The energy (2.13) for the energy densities given above is

$$\begin{aligned} F = \frac{1}{2}\int_0^{\frac{2\pi}{q_x}} \int_{-\frac{a}{2}}^{\frac{a}{2}} \Bigg[& B_0\left(u_{,z} - \frac{1}{2}u_{,x}^2\right)^2 + B_2 u_{,xz}^2 \\ & - \mu_0 \Delta\chi H^2\left(u_{,x}^2\cos(2\theta) - u_{,x}(1+u_{,z})\sin(2\theta) + \sin^2\theta\right) \\ & + A_{12}u_{,xx}^2 + (B_{13} - C_1)u_{,xx}u_{,xz}\Bigg]\,\mathrm{d}z\,\mathrm{d}x \\ & + \frac{1}{2}\tau_0\omega\int_0^{\frac{2\pi}{q_x}} \left[\cos^2\theta - u_{,x}^2\cos 2\theta + u_{,x}(1+u_{,z})\sin(2\theta)\right]_{z=-\frac{a}{2}}\mathrm{d}x \\ & + \frac{1}{2}\tau_0\omega\int_0^{\frac{2\pi}{q_x}} \left[\cos^2\theta - u_{,x}^2\cos 2\theta + u_{,x}(1+u_{,z})\sin 2\theta\right]_{z=\frac{a}{2}}\mathrm{d}x, \end{aligned} \tag{2.14}$$

where an inconsequential constant contribution that has no dependence upon u and θ has been neglected.

It is known that for small values of the smectic cone angle θ we can employ the approximations [18]

$$A_{12} = K_1 + \bar{A}_{12}\theta^2, \qquad B_2 = \bar{B}_2\theta^2 \qquad B_3 = \bar{B}_3\theta^3, \qquad B_{13} = \bar{B}_{13}\theta^3 \qquad C_1 = \bar{C}_1\theta, \tag{2.15}$$

where the elastic constants K_1, $\bar{A}_{12}$, $\bar{B}_1$, $\bar{B}_2$, $\bar{B}_{13}$ and $\bar{C}_1$ are assumed to be only weakly temperature dependent. It is known *a priori* that K_1, $\bar{B}_1$ and $\bar{B}_2$ are positive [18]. We remark here that making these small θ approximations for the sinusoidal contributions, discarding constant contributions to the energy and taking the limit as $\theta \to 0$ reduces (2.14) to the expression for the free energy for SmA liquid crystals, namely

$$\begin{aligned} F = \frac{1}{2}\int_0^{\frac{2\pi}{q_x}} \int_{-\frac{a}{2}}^{\frac{a}{2}} & \left[K_1 u_{,xx}^2 + B_0\left(u_{,z} - \frac{1}{2}u_{,x}^2\right)^2 - \mu_0\Delta\chi H^2 u_{,x}^2\right]\mathrm{d}z\,\mathrm{d}x \\ & + \frac{1}{2}\tau_0\omega\int_0^{\frac{2\pi}{q_x}} \left[1 - u_{,x}^2\right]_{z=-\frac{a}{2}}\mathrm{d}x + \frac{1}{2}\tau_0\omega\int_0^{\frac{2\pi}{q_x}} \left[1 - u_{,x}^2\right]_{z=\frac{a}{2}}\mathrm{d}x. \end{aligned} \tag{2.16}$$

2.2. First variation of the free energy

We seek to minimize the free energy (2.14) and do so by employing the Gâteaux variation as outlined by Sagan [19, p 26]. Let $\mathcal{S}$ be a linear space over the field of reals R and denote the space of competing functions of admissible variations by $\Sigma \subset \mathcal{S}$ and $\mathcal{H} \subset \mathcal{S}$, respectively. We define the Gâteaux variation $\delta F[\eta]$ of $F[u]$ at $u = u_m$ by

$$\delta F[\eta] = \frac{\mathrm{d}}{\mathrm{d}\epsilon} F[u_m + \epsilon\eta]\bigg|_{\epsilon=0}, \tag{2.17}$$

where $\epsilon \in R$, provided the right-hand side exists for all $\eta \in \mathcal{H}$. A necessary condition for the functional $F[u]$ to assume a relative minimum in Σ at $u = u_m$ is that

$$\delta F[\eta] = 0, \qquad \text{for all} \quad \eta \in \mathcal{H}. \tag{2.18}$$

For clarity, we shall compute the variations of the bulk energy and the surface energy separately. We denote the bulk free energy by F_b and its associated integrand by $f_b(u_x, u_z, u_{xx}, u_{xz})$. The surface energy is represented by F_s with its associated integrand $f_s(u_x, u_z)$. By writing

$$\bar{u}(x, z) = u(x, z) + \epsilon\eta(x, z), \tag{2.19}$$

we have

$$\frac{\mathrm{d}}{\mathrm{d}\epsilon}F_b(\bar{u}) = \int_0^{\frac{2\pi}{qx}}\int_{-\frac{a}{2}}^{\frac{a}{2}} \frac{\mathrm{d}f_b(\bar{u})}{\mathrm{d}\epsilon}\,\mathrm{d}z\,\mathrm{d}x \tag{2.20}$$

$$= \int_0^{\frac{2\pi}{qx}}\int_{-\frac{a}{2}}^{\frac{a}{2}} \frac{\partial f_b}{\partial \bar{u}_{,z}}\frac{\partial \bar{u}_{,z}}{\partial\epsilon} + \frac{\partial f_b}{\partial \bar{u}_{,x}}\frac{\partial \bar{u}_{,x}}{\partial\epsilon} + \frac{\partial f_b}{\partial \bar{u}_{,xz}}\frac{\partial \bar{u}_{,xz}}{\partial\epsilon} + \frac{\partial f_b}{\partial \bar{u}_{,xx}}\frac{\partial \bar{u}_{,xx}}{\partial\epsilon}\,\mathrm{d}z\,\mathrm{d}x, \tag{2.21}$$

and so we can state

$$\frac{\mathrm{d}}{\mathrm{d}\epsilon}F_b(\bar{u})\bigg|_{\epsilon=0} = \int_0^{\frac{2\pi}{qx}}\int_{-\frac{a}{2}}^{\frac{a}{2}} \eta_{,z}\frac{\partial f_b(u)}{\partial u_{,z}} + \eta_{,x}\frac{\partial f_b(u)}{\partial u_{,x}} + \eta_{,xz}\frac{\partial f_b(u)}{\partial u_{,xz}} + \eta_{,xx}\frac{\partial f_b(u)}{\partial u_{,xx}}\,\mathrm{d}z\,\mathrm{d}x. \tag{2.22}$$

Employing integration by parts we can express the above as

$$\begin{aligned}\delta F_b[\eta] = {} & \left[\left[\eta\frac{\partial f_b}{\partial u_{,xz}}\right]_{z=-\frac{a}{2}}^{z=\frac{a}{2}}\right]_{x=0}^{x=\frac{2\pi}{qx}} + \int_0^{\frac{2\pi}{qx}}\left[\eta\left(\frac{\partial f_b}{\partial u_{,z}} - \left(\frac{\partial f_b}{\partial u_{,xz}}\right)_{,x}\right)\right]_{z=-\frac{a}{2}}^{z=\frac{a}{2}}\mathrm{d}x \\ & + \int_{-\frac{a}{2}}^{\frac{a}{2}}\left[\eta\left(\frac{\partial f_b}{\partial u_{,x}} - \left(\frac{\partial f_b}{\partial u_{,xz}}\right)_{,z} - \left(\frac{\partial f_b}{\partial u_{,xx}}\right)_{,x}\right) + \eta_{,x}\frac{\partial f_b}{\partial u_{,xx}}\right]_{x=0}^{x=\frac{2\pi}{qx}}\mathrm{d}z \\ & + \int_0^{\frac{2\pi}{qx}}\int_{-\frac{a}{2}}^{\frac{a}{2}}\eta\left(\left(\frac{\partial f_b}{\partial u_{,xz}}\right)_{,xz} - \left(\frac{\partial f_b}{\partial u_{,z}}\right)_{,z} - \left(\frac{\partial f_b}{\partial u_{,x}}\right)_{,x} + \left(\frac{\partial f_b}{\partial u_{,xx}}\right)_{,xx}\right)\mathrm{d}z\,\mathrm{d}x.\end{aligned} \tag{2.23}$$

Now consider, for the moment, the surface variation δF_s, which can be written as

$$\delta F_s[\eta] = \frac{\mathrm{d}}{\mathrm{d}\epsilon}F_s(\bar{u})\bigg|_{\epsilon=0}. \tag{2.24}$$

An evaluation of this variation for the surface integral given in (2.14) gives

$$\begin{aligned}\delta F_s[\eta] = {} & \frac{1}{2}\tau_0\omega\int_0^{\frac{2\pi}{qx}}[\eta_{,x}(\sin(2\theta)(1+u_{,z}) - 2\cos(2\theta)u_{,x})]_{z=-a/2}\,\mathrm{d}x \\ & + \frac{1}{2}\tau_0\omega\int_0^{\frac{2\pi}{qx}}[\eta_{,x}(\sin(2\theta)(1+u_{,z}) - 2\cos(2\theta)u_{,x})]_{z=a/2}\,\mathrm{d}x,\end{aligned} \tag{2.25}$$

which, upon an application of integration by parts, allows us to write the variation of the surface energy in the form

$$\begin{aligned}\delta F_s[\eta] = {} & \frac{1}{2}\tau_0\omega[[\eta(\sin(2\theta)(1+u_{,z}) - 2\cos(2\theta)u_{,x})]_{z=-a/2} \\ & + [\eta(\sin(2\theta)(1+u_{,z}) - 2\cos(2\theta)u_{,x})]_{z=a/2}]_{x=0}^{x=\frac{2\pi}{qx}} \\ & - \frac{1}{2}\tau_0\omega\int_0^{\frac{2\pi}{qx}}[\eta(\sin(2\theta)u_{,xz} - 2\cos(2\theta)u_{,xx})]_{z=-a/2}\,\mathrm{d}x \\ & - \frac{1}{2}\tau_0\omega\int_0^{\frac{2\pi}{qx}}[\eta(\sin(2\theta)u_{,xz} - 2\cos(2\theta)u_{,xx})]_{z=a/2}\,\mathrm{d}x.\end{aligned} \tag{2.26}$$

It follows that the total first variation is given by

$$\delta F[\eta] = \delta F_b[\eta] + \delta F_s[\eta]. \tag{2.27}$$

We now set $\Sigma \equiv \mathcal{H}$, where each $u, \eta \in \mathcal{H}$ are constrained to be periodic in x with period $2\pi/q_x$, even in z and have their derivatives with respect to z constrained to be odd in z. With these constraints placed upon u and η, it can be shown that the first term in (2.23), the integral with respect to z in (2.23) and the first term in (2.26) are equivalent to zero. It will be supposed further that a solution for the layer displacement can take the form [8, 9]

$$u(x, z) = u_0 \sin(q_x x)\cos(q_z z), \tag{2.28}$$

with q_x and q_z wave numbers and u_0 an arbitrary positive constant. Substituting this ansatz into the full variation, given by the sum of the bulk variation and the surface variation in (2.27), and making use of the constraints placed on η above, finally reveals the required first variation to be

$$\begin{aligned}\delta F[\eta] = u_0 \int_0^{\frac{2\pi}{q_x}} \int_{-\frac{a}{2}}^{\frac{a}{2}} \eta(x, z)\big[q_x q_z \sin(q_z z)\cos(q_x x)\big((B_{13} - C_1)q_x^2 + \mu_0 \Delta\chi H^2 \sin(2\theta)\big) \\ + \cos(q_z z)\sin(q_x x)\big(q_z^2(B_0 + q_x^2 B_2) + A_{12} q_x^4 - \mu_0 \Delta\chi H^2 q_x^2 \cos(2\theta)\big)\big]\,\mathrm{d}z\,\mathrm{d}x \\ + 2u_0 \int_0^{\frac{2\pi}{q_x}} \eta\left(x, \frac{a}{2}\right)\sin(q_x x)\left[\tau_0 \omega q_x^2 \cos(2\theta)\cos\left(\frac{a q_z}{2}\right)\right. \\ \left. - q_z \sin\left(\frac{a q_z}{2}\right)\left(B_0 + B_2 q_x^2\right)\right]\mathrm{d}x.\end{aligned} \tag{2.29}$$

We recall the requirement (2.18) to minimize the free energy. However, note that $\eta(x, z)$ is evaluated at $z = a/2$ in the single integral with respect to x that appears in the full variation (2.29). If we require $\delta F[\eta] = 0$ for all arbitrary $\eta \in \mathcal{H}$, then both of the integrands that appear in equation (2.29) must equate to zero independently. Therefore, assuming that η is not necessarily zero on the boundaries, we are forced into the requirements

$$q_x^2(C_1 - B_{13}) = \mu_0 \Delta\chi H^2 \sin(2\theta), \tag{2.30}$$

$$q_z^2 = \frac{q_x^2\big(\mu_0 \Delta\chi H^2 \cos(2\theta) - A_{12} q_x^2\big)}{B_0 + B_2 q_x^2}, \tag{2.31}$$

$$\tau_0 \omega = q_z q_x^{-2} \sec(2\theta)\tan\left(\frac{a q_z}{2}\right)\left(B_0 + B_2 q_x^2\right). \tag{2.32}$$

These three equations are in the three unknowns at criticality, namely H, q_x and q_z. We may set

$$\begin{aligned} &C_1 - B_{13} = 10^{-10}\ \mathrm{N}, \qquad A_{12} = 4 \times 10^{-12}\ \mathrm{N}, \qquad B_0 = 8.47 \times 10^6\ \mathrm{Nm}^{-2}, \\ &B_2 = 5 \times 10^{-12}\ \mathrm{N}, \qquad \theta = \frac{\pi}{6}\ \mathrm{rad}, \end{aligned} \tag{2.33}$$

as typical SmC material parameter values (cf [13]) in order to obtain the weak-anchoring critical threshold H_c and the accompanying wave numbers q_{xc} and q_{zc} at criticality via the numerical solution of the simultaneous equations (2.30)–(2.32). Plots of these numerical solutions can be seen in figure 2. Note that the critical field strength and both wave numbers tend to their respective classical strong-anchoring limit magnitudes as the anchoring strength tends to the 'infinite' strong-anchoring limit. Expressions in the strong-anchoring limit case are given in section 2.3. From these expressions, and the information given in figure 2, we can calculate the magnitude of the critical field strengths for SmC with weak surface anchoring, SmC with strong surface anchoring and SmA ($\theta \equiv 0$) with strong surface anchoring. They are $H_c \approx 1600\ \mathrm{A\,m^{-1}}$, $H_c \approx 3000\ \mathrm{A\,m^{-1}}$ and $H_c \approx 1250\ \mathrm{A\,m^{-1}}$, respectively.

In the weak-anchoring case the critical field threshold H_c can also be identified from a consideration of the energy. We can construct the energy difference $\Delta F = F(u(x,z)) - F(u \equiv 0)$ between the zero solution and the variable solution discussed above. As H increases above zero, the quantity ΔF will first reach zero when the system reaches criticality at the critical field magnitude H_c that will occur as the wave numbers also achieve their critical values q_{xc} and q_{zc}. Inserting the solution (2.28) and the zero solution into ΔF shows, after some calculation working to second order in u and its derivatives, that H_c, q_{xc} and q_{zc} must satisfy the relation

$$\mu_0 \Delta\chi H_c^2 \cos(2\theta) = A_{12} q_{xc}^2 + \left(B_0 + B_2 q_{xc}^2\right) \frac{q_{zc}^2}{q_{xc}^2} \left(\frac{aq_{zc} - \sin(aq_{zc})}{aq_{zc} + \sin(aq_{zc})} \right) - 4\tau_0 \omega \cos(2\theta) \frac{q_{zc} \cos^2(aq_{zc}/2)}{aq_{zc} + \sin(aq_{zc})}. \tag{2.34}$$

This relation is certainly satisfied whenever H_c, q_{xc} and q_{zc} satisfy equations (2.30)–(2.32): note that if we substitute for H_c^2 via the wave number requirement (2.31) in terms of q_{xc} and q_{zc} then condition (2.34) reduces to the corresponding requirement given by equation (2.32) at criticality. We also remark that the results in (2.31), (2.32) and (2.34) reduce to the forms given by Ishikawa and Lavrentovich [9] for a lamellar system with weak-anchoring conditions for cholesteric liquid crystals when θ is set to zero. Therefore the above results for the weak Helfrich–Hurault threshold H_c for SmC are natural extensions to those for SmA and other lamellar-like materials.

2.3. The strong-anchoring limit case

The strong-anchoring limit occurs as $\omega \to \infty$ in (2.32). This happens when q_z tends to the limiting value of π/a. Under these circumstances, the relation (2.31) gives an expression for the magnetic field magnitude in terms of the wave number q_x, given by

$$\mu_0 \Delta\chi H^2 \cos(2\theta) = q_x^2 A_{12} + B_2 \left(\frac{\pi}{a}\right)^2 + B_0 q_x^{-2} \left(\frac{\pi}{a}\right)^2. \tag{2.35}$$

The right-hand side of this expression can be minimized with respect to the wave number q_x in order to determine the critical field magnitude H_c at a critical value q_{xc} of the wave number for the onset of the Helfrich–Hurault transition. A straightforward calculation determines that

$$q_{xc}^2 = \frac{1}{\lambda}\frac{\pi}{a}, \qquad \text{with} \quad \lambda = \sqrt{\frac{A_{12}}{B_0}}, \tag{2.36}$$

where λ has been introduced as a typical length scale [13, p 289], analogous to that used by de Gennes and Prost [7] for SmA. Inserting q_{xc} into (2.35) shows that the critical field strength H_c is given by

$$\mu_0 \Delta\chi H_c^2 \cos(2\theta) = 2\pi \frac{A_{12}}{\lambda a} + B_2 \left(\frac{\pi}{a}\right)^2. \tag{2.37}$$

Using the approximations (2.15), we can take the limit as θ tends to zero to find that the classical threshold for SmA can be recovered, which may be expressed as [7, 13]

$$\mu_0 \Delta\chi H_c^2 = 2\pi \frac{K_1}{\lambda a}, \qquad \text{where} \quad \lambda = \sqrt{\frac{K_1}{B_0}}. \tag{2.38}$$

Thus the results in (2.31) and (2.32) for SmC liquid crystals are consistent extensions to those known for SmA under strong-anchoring conditions. The result for H_c in (2.37) also extends that which is known for SmC [8, 13] when terms involving u_{zz} in the energy integrand

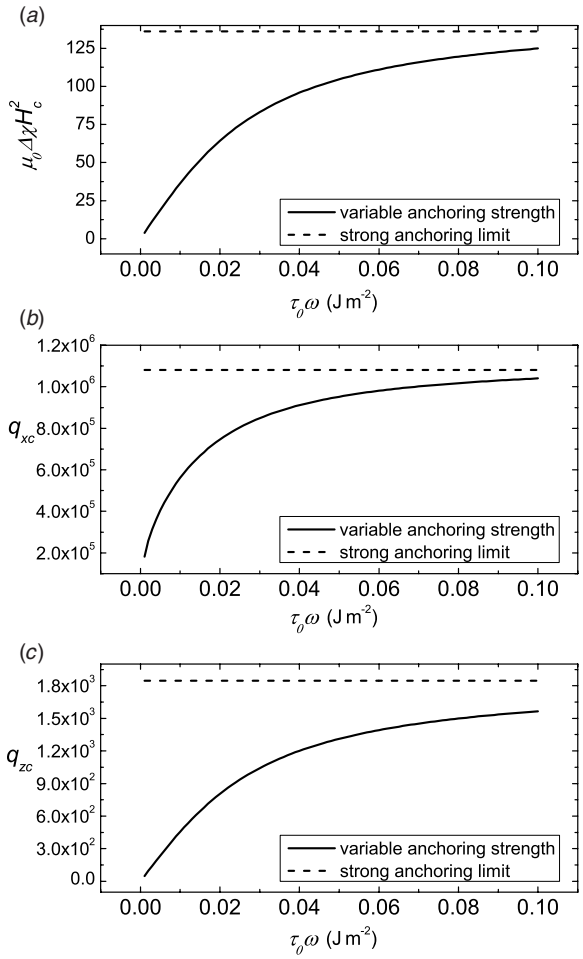

Figure 2. Plots showing the dependence of the critical field strength and wave numbers on the anchoring strength for the material parameter values given by (2.33). The plots for the variable anchoring strength (solid lines) tend towards the strong-anchoring limit cases (dashed lines) as the anchoring strength increases.

(which can appear after repeated integration by parts) are neglected; this neglection, which essentially leads to the omission of the B_2 contribution in (2.37), is considered valid in many circumstances by physical considerations because such terms will be dominated by the layer compression contribution $B_0 u_z^2$, as mentioned in [7, p 343].

3. Displacement of layers

In order to calculate an approximation for the displacement of the layers immediately above the critical magnetic field H_c, we retain the higher order terms of u and its derivatives in the free energy, which were ignored when obtaining the critical field strength; this procedure has been adopted elsewhere [9]. Substituting the ansatz (2.28) for u, we compute the difference

between the post-transitional free energy and the free energy at criticality. This is given by

$$F(H) - F(H_c) = \frac{3\pi u_0 \gamma B_0 q_x^3}{256 q_z} + \frac{\pi a}{q_x}\left(\sin^2\theta + \frac{1}{4}u_0^2\mu_0\Delta\chi\frac{q_x^2}{aq_z}\cos 2\theta(\sin aq_z + aq_z)\right)\left(H_c^2 - H^2\right), \tag{3.1}$$

where

$$\gamma = 4\cos^3\left(\tfrac{1}{2}aq_z\right)\sin\left(\tfrac{1}{2}aq_z\right) + 6\cos\left(\tfrac{1}{2}aq_z\right) + 3aq_z. \tag{3.2}$$

Minimizing this energy difference with respect to the layer undulation magnitude u_0 results in the solution

$$u_0 = \left(\frac{32}{3}\right)^{\frac{1}{2}}\left(\frac{\mu_0\Delta\chi H_c^2}{\gamma B_0 q_x^2}\cos(2\theta)(\sin(q_z a) + aq_z)\right)^{\frac{1}{2}}\left(\left(\frac{H}{H_c}\right)^2 - 1\right)^{\frac{1}{2}}, \tag{3.3}$$

which, upon using the relation given by equation (2.31), can be presented as

$$u_0 = \left(\frac{32}{3\gamma B_0}\right)^{\frac{1}{2}}\left(\left(\left(B_0 + B_2 q_x^2\right)\frac{q_z^2}{q_x^4} + A_{12}\right)(\sin(q_z a) + aq_z)\right)^{\frac{1}{2}}\left(\left(\frac{H}{H_c}\right)^2 - 1\right)^{\frac{1}{2}}. \tag{3.4}$$

In figure 3, we compare the results from the experiments presented in [9] with the classical SmA theory [1, 2, 7] and the layer displacement result given in (3.4). In order to compare the results legitimately, we have employed the material parameter values $B_0 = 0.44$ J m^{-3} and $K = 3.7 \times 10^{-7}$ N, as suggested for cholesterics [9] and assigned $a = 0.0017$ m as the depth of the cell. All other material parameter values used are given via (2.33) and the wave numbers are set as $q_x \approx 10^6$ m^{-1} and $q_z \approx 5 \times 10^3$ m^{-1}, which are realized from figure 2. Similarly, a comparison plot for the displacement amplitude using the classical theory and the revised theory presented here for typical smectic parameter values, given via (2.33), and the wave numbers given above, is presented in figure 4. We note here that the value of the elastic constant A_{12} given in (2.33) is an estimate, since measurements of the layer bending constants and the coupling constants are rare. We use the relation given in (2.15) to assume $A_{12} \approx K_1 = 4 \times 10^{-12}$ N. The results obtained show that whilst the layer displacement amplitudes of the revised SmC theory are of the same order of the classical SmA theory (and the cholesteric experimental results), we can clearly see, in both comparison plots, that the revised theory permits layer undulations of greater magnitude. This result is expected physically as the weak-anchoring energy allows greater flexibility of the layers and the director at the boundary than strong anchoring.

It is known, in the case of an applied electric field, that the above methodology will produce a mathematically analogous situation [10]. However, the recent experiments of Senyuk *et al* [10] have reported that as the magnitude of the electric field increases above the threshold value E_c the layer disturbances will exhibit sinusoidal undulations before going on to display periodic undulations that resemble Jacobian functions. Moreover, in very high field regimes, these structures will begin to be replaced by a complex arrangement of parabolic focal conic domain structures (PFCD) that are made up of parallel layers [10]. Such structures have been reported at values of $E/E_c \gtrsim 1.9$. The model that has been introduced in this paper for the undulation amplitude will be valid for fields that are just above the threshold value E_c. For the sinusoidal ansatz used above, the results in figures 3 and 4 are therefore expected to be analogously applicable to electric field effects for field magnitudes just above E_c. A fully nonlinear analysis, beyond the scope of this paper, is required in order to extend the model discussed in [10] for the transition to the PFCD structure. Such work would be of direct relevance to the situation for applied magnetic or electric fields.

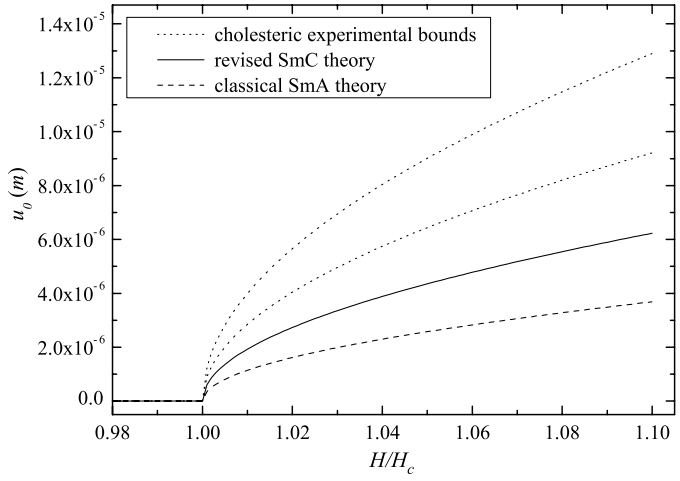

Figure 3. Comparison of the displacement amplitude u_0 immediately above H_c for the experimental results of Ishikawa and Lavrentovich [9] (dotted lines), the classical theory of SmA [1, 2] (dashed line) and the revised theory for SmC presented here (solid line). We see that the SmC case results in a layer displacement magnitude of the same order but below the upper and lower bounds for a typical cholesteric striped phase. The displacement for SmC is also greater than that for the classical Helfrich–Hurault effect in SmA. Here, for comparison with the previous results in [9], we have assumed $a = 0.0017$ m, $B = 0.44$ J m^{-3}, $q_x \approx 10^6$ m^{-1} and $q_z \approx 5 \times 10^3$ m^{-1}.

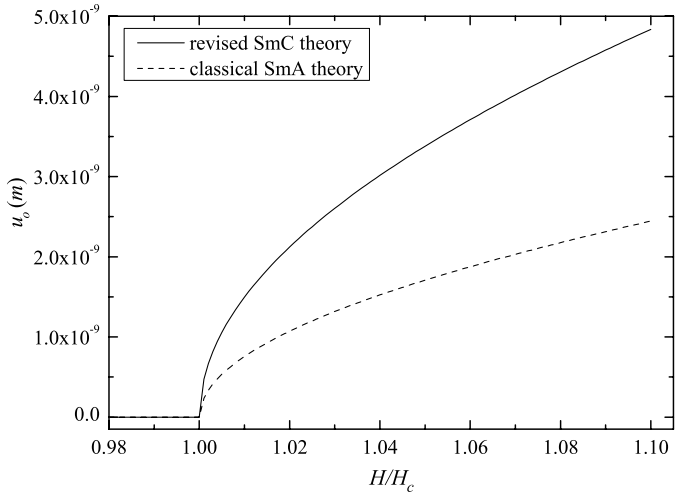

Figure 4. Comparison of the displacement amplitude immediately above H_c of the classical theory of SmA and the revised theory for SmC. Here, the typical smectic material parameter values given in (2.33) have been used, along with $a = 0.0017$ m, $q_x \approx 10^6$ m^{-1} and $q_z \approx 5 \times 10^3$ m^{-1}.

4. Discussion

This paper has considered a sample of smectic liquid crystal, confined between two semi-infinite plates, with weak anchoring on the cell boundaries. A magnetic field **H** is applied

parallel to the smectic layers, causing displacement of the layers when the magnitude of the field is above some critical threshold H_c. Using the Rapini–Papoular surface energy [17], and the previous methodology of Stewart [8], we have constructed a free energy which describes this system.

Minimizing the free energy using a Gâteaux variation, necessary requirements on the layer displacement function were found. Assuming a form for the layer displacement function allows us to state relations between the wave numbers describing the displacements, the elastic energies of the liquid crystal and the magnetic field strength. By employing these relations, along with the free energy and the supposed layer displacement ansatz, we have computed a form for the critical field strength and a relationship between the critical wave numbers. Illustrations showing the dependence of the critical field strength and critical wave numbers upon the anchoring strength (and consequently comparing the results with the classical strong-anchoring case) have been presented in figure 2. The effect that the anchoring strength has on the critical field strength (and wave numbers) is evident in these illustrations and the limiting magnitude of the aforementioned properties as the anchoring strength reaches 'strong-anchoring' proportions has been discussed in section 2.3. The Rapini–Papoular weak-anchoring surface energy, mentioned above, has been used here. Nevertheless, there are other theoretical models for weak-anchoring energies and there is scope for further investigation of weak-anchoring phenomena by comparing the results found when different surface energy potentials are used (e.g. [20–22]). The application of the minimizing technique used in section 2 is quite general and could be developed for such other anchoring potentials and smectic and lamellar models. Additionally, there are various other elastic energies available for smectic and related mesophases, such as those mentioned by Stallinga and Vertogen [23, 24], and these may also be deployed in a similar analysis.

The displacement of the layers immediately above the critical magnetic field H_c has been calculated in section 3 by minimizing the change in the free energy from the critical state to the post-transitional state. In doing so, we find a form for the layer displacement amplitude which is comparable to the displacement amplitude found from the classical Helfrich–Hurault theory [1, 2] and the experimental work in cholesteric liquid crystals carried out by Ishikawa and Lavrentovich [9] and Senyuk *et al* [10]. We can see from figure 3 that using material parameters suggested in [9] the amplitudes of the undulations in a SmC liquid crystal, while being of the same order, are greater than those estimated via the classical Helfrich–Hurault theory, yet lower than those calculated experimentally in [9] for a similar cholesteric system. Similar results are found when typical SmC parameter values, as suggested in [13], are used to compare the classical Helfrich–Hurault theory with the theory presented in this paper.

As mentioned in section 3, an application of an electric field to induce layer undulations well above threshold values has been carried out experimentally, and analysed in a similar fashion to that here and in [9], by Senyuk *et al* [10]. These authors also incorporated weak anchoring into their model. The transformation sequence from sinusoidal undulations to Jacobian function undulations and then to parabolic focal conic domains as the magnitude of the electric field is increased above the critical threshold has been observed experimentally in [10]. A similar transformation from sinusoidal undulations to focal conics has been discussed in [25–27]. The work in section 3 is directly relevant for magnetic or electric fields just above threshold and it remains as future work to carry out a fully nonlinear analysis of the sequence of layer disturbances that occur as the field magnitude increases. Critical electric fields have also been calculated by Bevilacqua and Napoli [28] for the Helfrich–Hurault effect in SmA under strong-anchoring conditions when taking into account the electro-mechanical coupling, which has been neglected in this paper. Such coupling may also be introduced in the model presented here for SmC with weak anchoring. Theoretical results for comparisons with data

appear to be scarce in the literature and it is hoped that the investigation contained in this paper will encourage more theoretical and experimental work which will attempt to ascertain the validity of many of the current modelling assumptions.

References

[1] Helfrich W 1969 *Phys. Rev. Lett.* **23** 372–4
[2] Hurault J P 1973 *J. Chem. Phys.* **59** 2068–75
[3] Fukuda J and Onuki A 1995 *J. Phys. II France* **5** 1107–13
[4] Singer S J 1993 *Phys. Rev.* E **48** 2796–804
[5] Stewart I W 1998 *Phys. Rev.* E **58** 5926–33
[6] Chandrasekhar S 1992 *Liquid Crystals* 2nd edn (Cambridge: Cambridge University Press)
[7] de Gennes P G and Prost J 1993 *The Physics of Liquid Crystals* 2nd edn (Oxford: Oxford University Press)
[8] Stewart I W 2003 *Liq. Cryst.* **30** 909–20
[9] Ishikawa T and Lavrentovich O D 2001 *Phys. Rev.* E **63** 030501
[10] Senyuk B I, Smalyukh I I and Lavrentovich O D 2006 *Phys. Rev.* E **74** 011712
[11] Leslie F M, Stewart I W, Carlsson T and Nakagawa M 1991 *Contin. Mech. Thermodyn.* **3** 237–50
[12] Orsay Group 1971 *Solid State Commun.* **9** 653–5
[13] Stewart I W 2004 *The Static and Dynamic Continuum Theory of Liquid Crystals* (London: Taylor and Francis)
[14] Oseen C W 1933 *Trans. Faraday Soc.* **29** 883–99
[15] Kléman M and Parodi O 1975 *J. Phys.* **36** 671–81
[16] Ishikawa T and Lavrentovich O D 1999 *Phys. Rev.* E **60** R5037–9
[17] Rapini A and Papoular M 1969 *J. Phys. Colloq.* **30** 54–6
[18] Carlsson T, Stewart I W and Leslie F M 1991 *Liq. Cryst.* **9** 661–78
[19] Sagan H 1992 *Introduction to the Calculus of Variations* (New York: Dover)
[20] Zhao W, Wu C and Iwamoto M 2002 *Phys. Rev.* E **65** 031709
[21] Belyakov V A, Stewart I W and Osipov M A 2004 *JETP* **99** 73–82
[22] Belyakov V A, Stewart I W and Osipov M A 2005 *Phys. Rev.* E **71** 051708
[23] Stallinga S and Vertogen G 1994 *Phys. Rev.* E **49** 1483–94
[24] Stallinga S and Vertogen G 1995 *Phys. Rev.* E **51** 536–43
[25] Pavel J and Glogarová 1991 *Liq. Cryst.* **9** 87–93
[26] Lavrentovich O D and Kléman M 1993 *Phys. Rev.* E **48** R39–42
[27] Findon A, Gleeson H and Lydon J 2000 *Phys. Rev.* E **62** 5137–42
[28] Bevilacqua G and Napoli G 2005 *Phys. Rev.* E **72** 041708